Techno-economic analysis on proton conductor ceramic based technologies for various materials, configurations, applications and products

Energy Conversion and Management 321 (2024) 119082

Contents lists available at ScienceDirect

Energy Conversion and Management

journal homepage: www.elsevier.com/locate/enconman

Techno-economic analysis on proton conductor ceramic based technologies for various materials, configurations, applications and products

Andrea Moranti [a,b,*], Julian Dailly [b], Massimo Santarelli [a], Federico Smeacetto [a]

[a] Politecnico di Torino, Corso Duca degli Abbruzzi 24, 10129 Torino, Italy
[b] European Institute for Energy Research, Emmy-Noether-Str. 11, 76131 Karlsruhe, Germany

ARTICLE INFO

Keywords:
Techno-economic analysis
Protonic ceramic cells (PCCs)
Hydrogen production/use
Energy storage
Solid state ammonia electrochemical synthesis

ABSTRACT

The increasing global energy consumption, particularly from fossil fuels, has led to environmental concerns linked with the increasing global Greenhouse Gas (GHG) emissions. Renewable energy sources offer a solution but are often intermittent and lack programmability. To tackle this issue, protonic ceramic cells (PCCs) are emerging as a promising technology and also as an alternative to traditional solid oxide cells (SOCs).

This study presents a techno-economic analysis of PCCs' systems for various applications and scenarios depending also on future scale up and improvements. Different materials, cell architectures, and configurations were considered.

The results, evaluated especially through economic indicators such as the levelized costs of the outputs, demonstrate the potential of PCCs as a clean and sustainable energy conversion technology. Positive results were reached with both current and improved future performances, finally comparing them with the ones of the current available SOCs technology.

1. Introduction

In the context of an increasing world's energy consumption [1] and considering the exploitation of renewable energy sources as a solution, technologies able to balance electrical power consumption, storage, and production have to be employed to tackle the issues of intermittency and lack of programmability [2], also to produce chemical products in a greener and more sustainable approach.

Looking at the available technologies, and focusing on the electrochemical route, protonic ceramic cells (PCCs) are gaining increasing attention. Originally studied in 1980 [3], the employed materials show high proton conductivity at moderate temperatures, between 400 and 600 °C, allowing for a cost-effective operation [4]. As for other high-temperature technologies, an efficiency higher than the low-temperature operating cells can be obtained [5] despite an increased degradation which in the long term may affect the cell's efficiency in both electricity and chemical product operation. The PCCs, in comparison with SOCs, present some advantages. Firstly, lower activation energy due to hydrogen ions (H^+) motion through the membrane instead of oxygen ones (O^{2-}), allowing faster reaction rates as well as requiring lower operating voltages. Furthermore, hydrogen and water remain separated during the operation avoiding fuel dilution in fuel cell (FC) mode and simplifying the treatment unit in electrolysis (EL). Due to lower operating temperature, higher theoretical efficiency, and lower requisites for the Balance of Plant (BoP) allowing for the exploitation of less valuable materials, are obtained. A higher resistance to H_2S poisoning is also observed, decreasing the requirements for desulphurization of the fuel making it suitable for alternative fuels. The operating conditions also allow to reduce the degradation, and related stack replacement, maintaining high efficiencies. However, disadvantages such as challenges in the anodic and cathodic reaction processes, sintering, conductivity, stability, durability, and scale up of the cells are found [6].

Overall PCCs are expected to allow cost-effective applications in

Abbreviations: ASR, Area specific resistance; ASU, Air separation unit; BoP, Balance of Plant; CC, Combustion chamber; EIS, Electrochemical impedance spectroscopy; EL, Electrolysis; EPCC, Engineering, Procurement, and Construction; FC, Fuel cell; FU, Fuel utilization; LCOA, Levelized cost of ammonia; LCOE, Levelized cost of electricity; LCOH, Levelized cost of hydrogen; LMTD, Logarithmic mean temperature difference; MEA, Membrane-electrode assembly; NPV, Net Present Value; PCCs, Protonic Ceramic cells; PCFC, Protonic ceramic fuel cell; RR, Recirculation rate; SOCs, Solid oxide cells; SRU, Single repeating unit; WACC, Weighted average cost of capital.

* Corresponding author at: Politecnico di Torino, Corso Duca degli Abbruzzi 24, 10129 Torino, Italy.
E-mail address: andrea.moranti@polito.it (A. Moranti).

https://doi.org/10.1016/j.enconman.2024.119082
Received 24 July 2024; Received in revised form 13 September 2024; Accepted 17 September 2024
Available online 25 September 2024

traditional electrolysis and fuel cell applications. Additionally, they are expected to enable the development of innovative sensor devices with increased sensing capabilities [7], and facilitate hydrogen separation and pumping to obtain high purity hydrogen from the water–gas shift, steam methane reforming, and pyrolyzed ethane [8,9]. Finally, they also allow the conversion of electricity into multiple chemical products (e.g. ammonia, methane) and vice versa [10,11].

The low technological readiness level implies a current focus on materials, single cells, or small stacks [5]. The scale-up and commercialization may be driven by the definition of standardized materials and production processes to decrease the cost even below the SOCs one [6].

Regarding this final issue, the research is currently converging toward similar electrolyte materials [3]. Through various doping strategies consisting of variable combinations of zirconium and cerium content as well as yttrium and ytterbium exploitation, significant advancements have been made in the optimization of the material's structure and defect chemistry with the improvement of the ionic conductivity of proton-conducting oxides. The presence of ytterbium, in addition to the improvement of the conductivity, was also found to improve the sinterability [12–14]. In addition to ytterbium, which has already been developed especially in the last fifteen years, also additional rare earth elements and transition metals have been found to improve ionic conductivity and thermal stability. Due to these increased performances, stacks composed of three cells have also obtained power densities of 0.42 W/cm^2 and 0.24 W/cm^2 respectively when fed by hydrogen and methane at 0.75 V at 550 °C were obtained and increased to 0.70 W/cm^2 at 600 °C. Maximum values of 1.398 W/ cm^2 at 700 °C were also observed [12]. These improvements were reached with the exploitation of improved material characterization, to better understand performance and stability, coupled with higher process control during fabrication [12,13]. Despite the positive achievements, technological bottlenecks can be found in both manufacturing and operation. Linked to the manufacturing there are issues related to the synthesis in terms of requirements for high temperature sintering and negative effects on its homogeneity. From the operation point of view issues related to chemical stability and degradation, especially in humid atmospheres, with corresponding negative effects on long term operation and durability, are present [12–14]. Thirdly, the chemical and thermal expansion of these materials can lead to higher stresses. Finally, the transition from laboratory scale synthesis to commercial production remains a challenge, due to a lack of uniformity in material properties and cell structure across different batches. Current developments from the material point of view have found BCZY and BCZYYb electrolytes as the most explored compositions especially from the year 2010 to date [12,13]. From the electrode point of view, literature is still focusing on a considerable number of materials and compositions with a focus, especially in this work, on BSCF and LSCF [14].

Furthermore, the typical technology used is the electrode-supported one, with the hydrogen electrode providing structural support to the cell, also allowing the reduction of the electrolyte layer thickness with the related decrease in resistance and voltage drop.

The combination of materials assumed for this work, according also to the considered references, are respectively: Ni-BZCY|BZCY|BSCF-BZCY [15–20], Ni-BZCY|BZCY|LSCF-BZCY [21–25], Ni-BZCYYb|BZCYYb|LSCF-BZCYYb [26–31], 25Ni10Ce-BCZYZ/BCZYZ/25FE-BCZYZ only for ammonia production from hydrogen injection [32], LSCF|BZY|LSCF only for ammonia production from water injection [33].

As already introduced, though, most of the available research is focused on a cell and SRU level, with the most promising planar cells in terms of active areas reached by Pirou et. Al [34], Dailly et al. [18], and J. Braun et al. [35] with the first compatibility with stack packaging carried out by Le et al. [13].

Less focus has been applied on a system level, which includes also the balance of plant (BoP), with only specific applications studied such as operation in fuel cell mode by Ferguson et al. [36], in electrolysis mode by Robert J. Kee [37] or green ammonia production by Morgan et. Al [38]. Under the aspect linked to the scaling up, there is a strong push towards optimization of synthesis methods for large scale production while maintaining material integrity and performances. Also, stack integration and integration in energy systems, are currently the most common trend both domestically and internationally, to create hybrid energy solutions coupled with renewable energy sources. Finally, there is also increased emphasis on the environment with the inclusion of abundant raw materials and environmentally friendly synthesis methods [12,13].

In this study, a detailed techno-economic analysis of the different membrane electrode assembly (MEA) materials, BoP and output products, such as electricity, hydrogen, and ammonia, is carried out by exploiting Excel and Python as tools. The main economic indicators are evaluated according to assumptions in terms of cell performances and scale up, also comparing them with those for the current SOCs technology employed. Finally, for each system, a sensitivity analysis using the validated model is performed to assess the most impacting operating parameters providing suggestions for future research and the scale up of the technology. The aim of this work, therefore, is to give focus to specific applications for this technology which still have not highly been carried out due to its low technological readiness. By focusing on multiple operating parameters and assessing not only the technological effect but especially the economic one, this research wants to contribute to the research and industrial sector, towards an economically sustainable development of this technology improving its competitiveness with respect to other available alternatives.

2. Materials and methods

2.1. Stack structure

As already mentioned, the main element varied in the cells considered in this study is the MEA. Its general structure consists of a central membrane, in this work selected between BZCY and BZCYYb, with two electrodes applied to its interface. In the so-called fuel electrode, composed of Nickel mixed with the electrolyte material, hydrogen, injected or produced, is found. On the other hand, on the opposite side of the membrane, the steam electrode, manufactured with a combination of LSCF and BSCF with electrolyte powder, is located. The MEA is then combined with other elements, such as adhesion and blocking layers, current collectors, sealants, and interconnectors, to create the single repeating unit (SRU).

Multiple single repeating units are finally combined into a stack to provide higher output power. One hundred SRU per stack are assumed in this work according to the commercial stack used as reference [39]. Multiple stacks can finally be combined into modules to reach the production required for the specific application.

2.2. Systems analyzed

The systems evaluated, and the corresponding models created, are respectively:

1) Two configurations in fuel cell mode:
a) *without H_2 recirculation and with flue gases for pre-heating.* The unreacted hydrogen at the outlet of the stack, due to the non unitary fuel utilization (FU), is routed in a combustion chamber with air and combusted recovering the thermal energy deriving from its combustion (see Fig. 1a).
b) *with H_2 recirculation and both electric heater and flue gas recirculation for pre-heating.* A portion of the unreacted hydrogen is recirculated into the system, while the remaining portion is injected into a combustion chamber. The flue gases are used for a dual purpose: air preheating to reduce the power requested by the electric heater and contribute to district heating (see Fig. 1b).

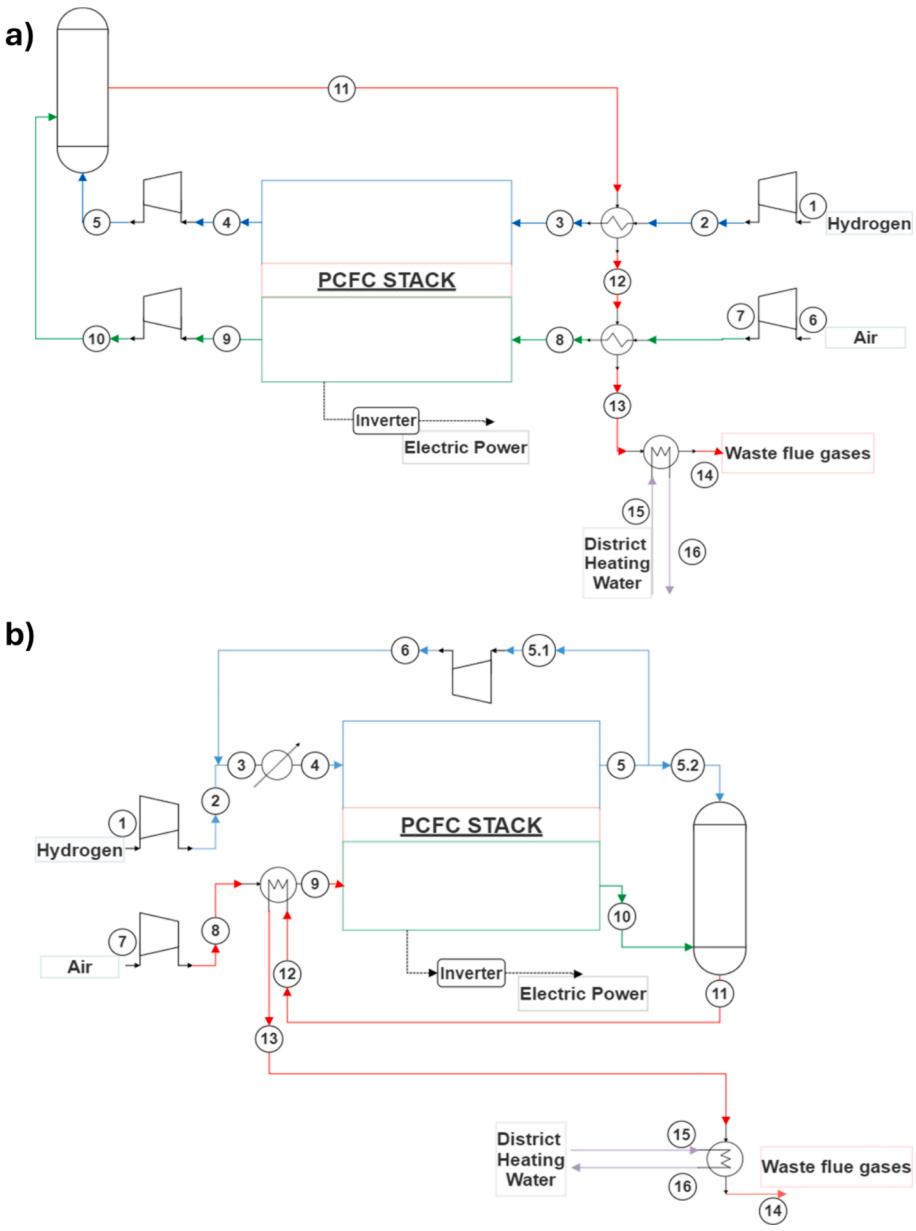

Fig. 1. Modeled Protonic ceramic fuel cell (PCFC) systems a) without H2 recirculation and with flue gases recirculation for pre-heating b) with H2 recirculation and both electric heater and flue gases recirculation for pre-heating.

All systems operate under these conditions: fuel cell stack runs at 600 °C and atmospheric pressure, fed by a mixture of 99.99 % H_2 and 0.01 % H_2O on the fuel electrode side, with a small amount of water introduced for computational requirements. On the air electrode side, regular air with 21 % oxygen and 79 % nitrogen feeds the stack.

Inlet temperature in the stack in baseline condition is set according to the literature [37]. Pressure losses through the system are 2 kPa and 3 kPa on the hydrogen and air side, 5 kPa in the heat exchangers, and 10 kPa in the combustion chamber. A 78 % compressor efficiency and 95 % heat exchanger efficiency are considered [38]. Finally, a fourth generation DH system is also examined.

2) One configuration in the electrolysis mode.

An optimized system's internal heat recovery process, originally optimized using pinch analysis was performed to find the most efficient way to transfer heat within the system minimizing the need for extra heating from electric heaters and solving the lack of explicit references. While different operating conditions and material flows might require pinch point temperature and heat exchanger configuration adjustments, this study has kept the same configuration for the different heat exchangers, corresponding to the one shown in Fig. 2 and evaluated in the baseline scenario, just partially modifying some of the flow rates when required.

The stack operates at 600 °C and atmospheric pressure under thermoneutral voltage and it is fed with a sweep gas composed entirely of hydrogen (99.99 %), to keep the advantage of pure hydrogen production. The opposite electrode utilizes a mixture of 90 % water (H_2O) and 10 % oxygen (O_2). The dilution through pure oxygen allows for the recovery of a fraction of the warm stream, that would otherwise be lost, also saving some energy required for pre-heating. To maintain a sufficient flow of the sweep gas (hydrogen) the system recirculates 10 % of the produced hydrogen also applying a slight overpressure. The same assumptions for pressure drop components efficiencies and DH systems as in the FC mode have been considered.

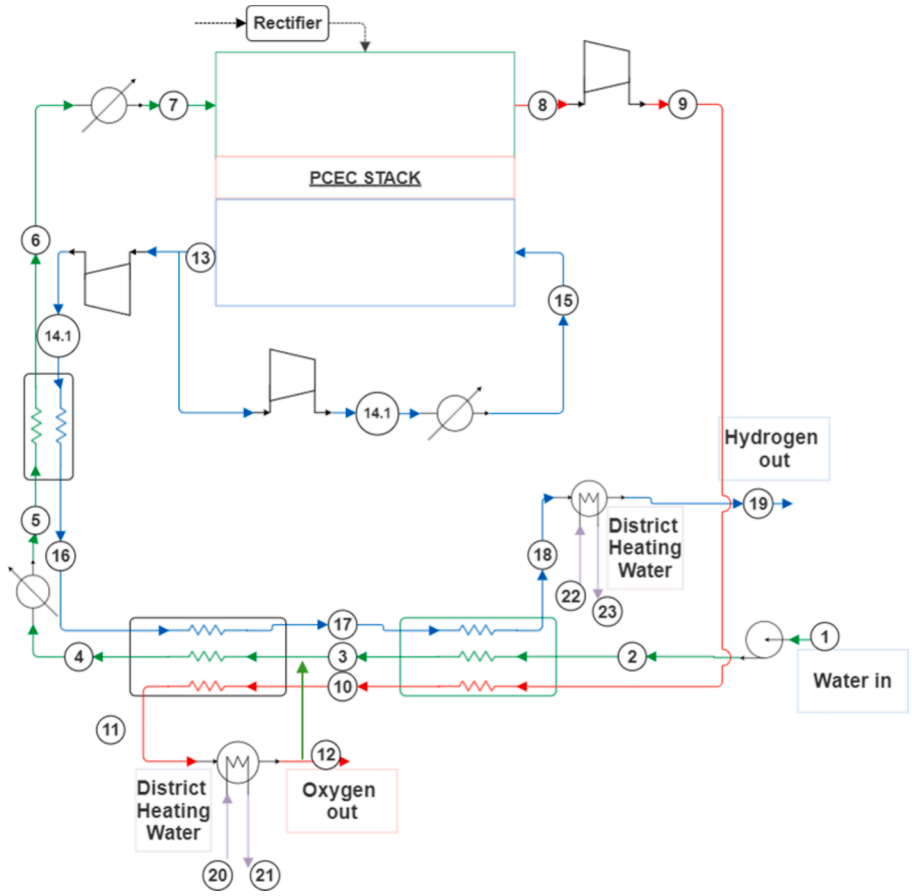

Fig. 2. Modeled Protonic ceramic electrolyzer cell system.

3) Two configurations for ammonia production (a chemical used in several applications [40]):
   a) *Injection of hydrogen in the stack*, previously produced with a separate electrolyzer and then mixed with additional water (see Fig. 3a).
   b) *Direct injection in the stack of water,* avoiding preliminary hydrogen production and simplifying the system (see Fig. 3b).

Reacting nitrogen is extracted from air via a cryogenic air separation unit (ASU), whose general scheme of the plant, and fluids' operating conditions, have been determined from available literature [41].

Also, an ammonia liquefaction system has been used to remove the produced ammonia from the hydrogen and nitrogen mixture via liquid and gaseous phases separation, employing an intercooled compression and expansion in a flash tank.

Finally, to separate hydrogen from other gases, and hybrid Pressure Swing Adsorption and membrane separation system has been considered using directly the results available in literature by Lin et. al [42]. Any slight hydrogen remaining is not considered a problem because it will convert into ammonia due to thermodynamics when inside the stack. The ammonia produced from this process is not considered because assumed as negligible.

2.3. Gas modeling

To obtain more accurate results, the dependence of fluids' physical and chemical properties on operating conditions such as temperature and pressure has been considered. Shomate Equations along with coefficients from the NIST database are used to evaluate molar heat capacities, standard enthalpy and standard entropy [43].

In addition to these properties, the compressibility factor, which describes how a gas deviates from ideal gas behavior, is estimated via Redlick-Kwong equations which involve a polynomial equation of third order [44].

2.4. Cell performances modeling

Due to the significant heterogeneity in material composition, layers thicknesses, and resulting performance of this technology, a detailed literature review is carried out further extrapolating as a key performance indicator the area specific resistance (ASR). This procedure has been conducted considering polarization curves and electrochemical impedance spectroscopies (EIS). The average value for the ASR of each source is finally used in combination with the standard deviation to evaluate the uncertainty and extrapolate the best- and worst-case scenario to use in the sensitivity analysis performed.

The corresponding ASR values are summarized in Table 1.

For ammonia synthesis only one reference for each system, respectively by Klinsrisuk et al. [32] for the hydrogen and water fed stack and from Yun et al. [33] for the water fed stack, are considered for polarization curve, faradaic efficiency, and operating conditions extrapolation.

The choice has been made by selecting materials as close as possible to those commonly used for hydrogen production while avoiding specific catalysts.

2.5. Stack modeling

The stack is assumed to be composed of 100 SRU, with a lifetime of five years, after which it must be substituted. The number of stacks is instead chosen to get a total net power, derived from the summation of the production of each one of them, approximately equal to 30 kW in

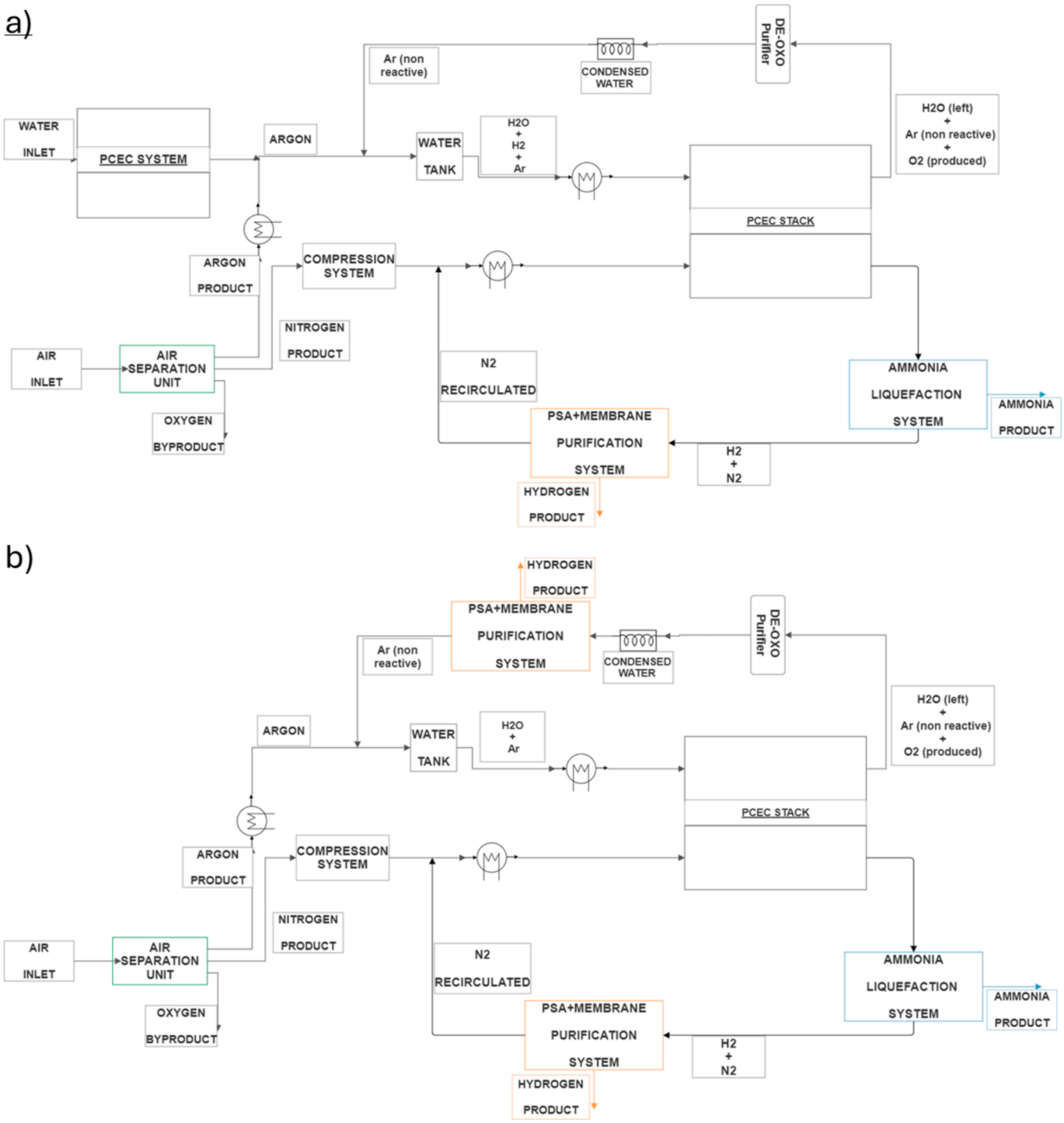

Fig. 3. Modeled ammonia synthesis systems a) Injection in the stack of hydrogen and water b) Direct injection in the stack of water.

fuel cell mode and 45 kW and 100 kW respectively for hydrogen and ammonia production.

2.6. Balance of plant technical modeling and economic assessment

Besides the stack, the BoP includes all components needed for the system to operate properly. For each component, a technical assessment is originally conducted and then, according to the evaluated requirements, the corresponding costs are estimated by applying Turton's function [45]. The purchase cost of the equipment, if operating at ambient temperatures and pressures, is therefore defined according to the equation [1].

$$\log_{10} C_p^0 = K_1 + K_2 \log_{10}(A) + K_3 [\log_{10}(A)][-] \quad (1)$$

The values for K_1, K_2, and K_3 are tabulated while A represents the size parameter for the different components.

The value of C_p^0 extrapolated is also corrected to obtain the bare module (C_{BM}), which accounts for different materials and operating conditions. Components such as combustion chamber (CC), heat exchangers, vessels or pumps are evaluated according to Equation [2].

Table 1
Fuel cell and electrolyzer cell performances.

Temperatures [°C]	Operating mode	Materials / ASR (Ωcm^2)		
		LSCF-BZCY	BSCF-BZCY	LSCF-BZCYYb
500	FC	–	2.47 ± 0.76	1.98 ± 0.54
	EL	–	1.73 ± 0.49	1.17 ± 0.32
550	FC	1.46 ± 0.34	2.05 ± 0.46	1.25 ± 0.24
	EL	1.06 ± 0.27	1.43 ± 0.29	0.74 ± 0.14
600	FC	1.17 ± 0.36	1.30 ± 0.42	0.84 ± 0.27
	EL	0.86 ± 0.29	0.91 ± 0.27	0.50 ± 0.16
650	FC	0.78 ± 0.20	0.79 ± 0.06	0.59 ± 0.29
	EL	0.57 ± 0.16	0.54 ± 0.04	0.35 ± 0.17
700	FC	0.46 ± 0.19	0.60 ± 0.11	0.43 ± 0.22
	EL	0.34 ± 0.16	0.42 ± 0.09	0.26 ± 0.13

$$C_{BM} = C_p^0\left(B_1 + B_2 F_M F_p\right)[\$] \tag{2}$$

where F_M is the material factor, depending on the listed identification number, whilst B1 and B2 are tabulated values which can all be found in the Turton's tables [45]. Operating pressures different from the atmospheric ones are finally accounted for by the parameter F_P which is for most components with equation [3] while for the vessel as equation [4].

$$\log_{10}F_p = C_1 + C_2\log_{10}P + C_3(\log_{10}P)^2[-] \tag{3}$$

$$F_{Pvessel} = \frac{\frac{(P+1)D}{2[850-0.6(1+P)}+0.00315}{0.0063}[-] \tag{4}$$

with P being the pressure in the bar gauge, C_1, C_2, and C_3 tabulated coefficients, and D the vessel diameter.

In addition, the bare module cost is rescaled when the size parameter is outside of the accepted range, using different rescaling factors (n) for the different components according to equation].

$$\frac{C_1}{C_0} = \left(\frac{S_1}{S_0}\right)^n[-] \tag{5}$$

Finally, the time shift concerning the reference year of 2001 used for the evaluation of the equations' coefficients, is performed with the CEPCI indicator with values in 2001 and the first semester of 2023 respectively equal to 397 and 801.4 [46] using the equation:

$$\frac{C_1}{C_0} = \frac{CEPCI_1}{CEPCI_0}[-] \tag{6}$$

2.6.1. Compressors

Component employed for fluids recirculation, selected according to the flow rates and pressures that cell or stack require for a proper operation. In the modeling process, isentropic compression was considered factoring in energy losses within the compressor using efficiency values (η_{iso}). The power is evaluated using equation [7].

$$\dot{W}_{comp} = \dot{m}\cdot\frac{k}{(k-1)\eta_{iso}}\cdot\frac{ZRT_{in}}{MW_{gas}}\cdot\left[\left(\frac{P_{out}}{P_{in}}\right)^{\frac{k-1}{k}}-1\right][W] \tag{7}$$

with $\dot{m}$ as mass flow rate in kg/s, k heat capacity ratio, R ideal gas constant in J/(mol K), MW_{gas} molecular gas weight in g/mol, T_{in} gas temperature at the inlet of the compressor in Kelvin and p_{in} and p_{out} the inlet and outlet pressures of the compressor in bar. The outlet temperature is then evaluated adding to the inlet temperature the value of the specific work divided by the specific heat capacity. An iterative approach is used to find the solution

For cost estimation, Turton's functions coefficients for "Centrifugal, axial and reciprocating compressors" were applied. These have been selected as more general than the rotary one, assuming carbon steel due to the low operating temperature and due to no chemical limitations except for stainless steel in ammonia production.

2.6.2. Heat exchangers

Component which allows the management of temperature of fluids either heating up or cooling down fluids allowing for both internal heat recovery as well as heat exchange with the external environment. The output of the technical analysis, required for the cost evaluation, is the heat exchanger surface (A) evaluated according to equation 8 based on factors like heat flux, global heat transfer coefficient [47] and logarithmic mean temperature difference (LMTD) which in counter flow configuration is defined from equation (9).

$$A = \frac{\dot{Q}}{U\cdot LMTD}[m^2] \tag{8}$$

$$LMTD = \frac{(T_{hin}-T_{cout})-(T_{hout}-T_{cin})}{\ln\left(\frac{T_{hin}-T_{cout}}{T_{hout}-T_{cin}}\right)}[-] \tag{9}$$

The inlet and outlet temperatures for the hot (T_h) and cold (T_c) fluids in Kelvin, are evaluated from Pinch analysis employing a Python script to optimize internal heat recovery. The cost estimation itself utilizes Turton's function coefficients for "Double pipe heat exchangers" in FC and EL mode, and "Floating head" in chemical processes such as ammonia synthesis, taking into account the advantages and disadvantages of the different technologies [42] and selecting carbon steel for fuel cell and electrolysis operation while stainless steel for ammonia synthesis. Finally, the values for the global heat transfer coefficient have been assumed depending on the fluids flowing at the two sides of the solid material according to available references [47].

2.6.3. Inverter and rectifier

Evaluated from an economic point of view exploiting the relationship, defined by Jamshidi et al. [48], between investment cost (IC) and electric power, depending on the specific cost assumed for this work equal to 120 $/kW. This component is assumed to be substituted every 10 years also due to its connection to a photovoltaic plant which is supposed to reduce its life [49,50]. As a simplification also the cost of the rectifier is assumed to be equal to the inverter one.

2.6.4. Vessels

The systems rely on various tanks and vessels for several functions including afterburners, air separation unit, and ammonia liquefaction system. To determine the appropriate volume for each vessel, firstly the fluids' properties at the inlet and outlet of the vessels are defined. For the outlet conditions of the combustion chamber, specifically, the chemical composition is evaluated assuming a complete combustion reaction between hydrogen and oxygen, according to equation (10), leaving residual oxygen and nitrogen, as well as the NOx, produced.

$$m_{H_2}h_{H_2} + m_{air}h_{air} = m_{fumes}h_{fumes} + m_{H_2}LHV_{H_2}(1-\eta_{CC}) \tag{10}$$

From the gas composition, the specific heat capacity of the stream can be calculated and used to define the outlet temperature of the flue gases from energy balance, accounting for inlet and outlet streams and also energy from combustion in the CC. Regarding the ASU vessels the inlet and outlet operating conditions are extrapolated from the available literature [41].

Foremost, knowing the mass flow rate as well as inlet and outlet

densities the average volumetric flow rate, and finally the vessel volume, can be evaluated. For the distillation columns of the ASU specific equations (11) and (12), have been employed.

$$D_c = \sqrt{\frac{4V_w}{\pi \rho_v u_v}} \tag{11}$$

$$u\_v = \left(-0.17l_t^2 + 0.27l_t - 0.047\right)\left[\frac{\rho_l - \rho_v}{\rho_v}\right] \tag{12}$$

When it comes to cost estimation, stainless steel is assumed as the material for all these vessels. This choice is driven by the high temperatures involved, particularly in the afterburner, and the potential for chemical reactions that might occur.

2.7. Economic assessment

The indicators used to assess the economic performances are summarized in this section.

2.7.1. Levelized cost

Defined for electricity (LCOE), hydrogen (LCOH) and ammonia (LCOA), this indicator determines the product's price to recover all the expenses, including initial investment and operational cost during the plant lifetime, useful to compare systems characterized by different technologies, sizes, lifespan, risks. The equation to determine this parameter is,

$$LCOE = \frac{C_0 + \sum_{t=1}^{N} \frac{C_{o\&m,t}}{(1+r)^t} + \sum_{t=1}^{N} \frac{(C_{f,t} - I_{DH,t})}{(1+r)^t}}{\sum_{t=1}^{N} \frac{E_{G,t}}{(1+r)^t}} [€/\text{kWh}] \tag{13}$$

$$LCOH = \frac{C_0 + \sum_{t=1}^{N} \frac{C_{o\&m,t}}{(1+r)^t} + \sum_{t=1}^{N} \frac{(C_{E,t} - I_{DH,t})}{(1+r)^t}}{\sum_{t=1}^{N} \frac{H_{G,t}}{(1+r)^t}} [€/\text{kg}_{\text{H2}}] \tag{14}$$

$$LCOA = \frac{C_0 + \sum_{t=1}^{N} \frac{C_{o\&m,t}}{(1+r)^t} + \sum_{t=1}^{N} \frac{(C_{E,t} - I_{DH,t} - I_{H2,t})}{(1+r)^t}}{\sum_{t=1}^{N} \frac{A_{G,t}}{(1+r)^t}} [€/\text{kg}_{\text{NH3}}] \tag{15}$$

with C_0 initial investment, $C_{o\&m,t}$ operation and maintenance expenditures, $C_{f,t}$ eventual fuel expenditures, $I_{DH,t}$ incomes from DH, $I_{H2,t}$ incomes from hydrogen, $E_{G,t}$ electricity produced, $H_{G,t}$ hydrogen produced, $A_{G,t}$ ammonia produced. Finally, t is the reference year while N is the number of years in the lifetime. All of the expenses and incomes are expressed in euros, the electricity produced in kWh and finally the chemical products in kg.

2.7.2. Net present value

Indicator useful to assess the profitability of the investment, which occurs if the NPV is higher than zero at the end of life of the plant. It can be evaluated with the equation.

$$NPV = -C_0 + \sum_{t=1}^{N} \frac{R_{WT,t} - C_{o\&m,t}}{(1+r)^t} [€] \tag{16}$$

with the newly introduced variable $R_{WT,t}$ representing the revenues in euros at the time interval t in years.

2.7.3. Weighted average cost of capital

Used for all previous equations as a discount rate it can be evaluated as

$$WACC = K_e \cdot \frac{E}{D+E} + K_d \cdot \frac{D}{D+E} [\%] \tag{17}$$

with $K_e = R_f + R_s + \beta\left(R_m - R_f\right)$ cost of equity affected by systemic risk of the investment (R_f), market return (R_m), β sensitivity of an investment and small stock premium with reduced capital (R_s) and $K_d = IRS + spread$ as cost of debt and IRS interest swap rate. D and E finally represent the amount of the investment financed with debt or equity. A final value of 6.6 % has been assumed for the WACC as calculated and also as confirmed by KPMG for the 2023.

2.7.4. National energy technology laboratory Method

The methodology employed by the National Energy Technology Laboratory to assess the final cost of a plant to be used in a techno-economic study which, starting from the initial investment, allows to take into account the cost of the core services provided by the contractor, estimating the Engineering-Procurement-Construction cost (EPCC) with an assumed increase of 8 %. Additional contingencies and owner's costs are considered in the Total Plant Cost (TPC) obtained by further increasing the EPCC by 20 %. Finally, the Total Ownership Cost (TOC) is estimated with a final overall increase of 20.20 % [51].

2.8. Validation

The modeled components have been validated through other studies available in the literature with several approaches. Firstly each single component has been validated. This has been made exploiting references related to PCEC, SOEC, ammonia synthesis but also different applications such as ASU [36,38,41,52–55]. The approach used consisted in assuming the operating conditions as those used in the cited sources, extrapolating the power consumed, the streams conditions at the outlet or any additional characteristic parameter of each component, verifying deviations lower than 5 %. A second approach, still related to the single components, is mostly linked to the economic aspects and performs again a comparison between the costs that were evaluated in this work and those found in different sources [38,52,56]. The third validation approach performs a comparison mainly on a system level, comparing specific energy consumptions [53,57]. The third and final validation is performed on the final outcomes by comparing the available literature with the results especially when same assumptions are used.

2.8.1. Economical assumptions and sensitivity analysis

To quantify the impact that each operating parameter has on the techno-economic performance of the systems, also to highlight what to focus on during the development and scale up of the PCCs technology, sensitivity analysis with respect to the baseline condition has been performed using the values summarized from Tables 2 to 4.

For the cost of the stack a study from literature benchmarking the expected stack manufacturing cost for proton conductor ceramic stacks has been used as a reference but also maintaining conservative values according to the current commercial price for SOCs, especially for the ammonia production plant for which the highest of the costs has been selected [58]. For electricity, the average selling price in fuel cell mode is selected according to Eurostat's electricity price statistics in the first quarter of 2023. The price for the heat recovered as district heating is instead assumed as equal to 0.06 €/kWh [59].

The cost of electricity for hydrogen and ammonia production is based on Power Purchasement agreement prices [60] in the EU in the first quarter of 2023. The LCOH for currently available technology for

Table 2
Values used for sensitivity analysis in fuel cell mode.

Modified parameter	Baseline	Best case	Worst case
Stack cost [€/kW]	500	300	700
Purchase hydrogen cost [€/kg]	3.8	1.95	5.95
Selling electricity price [€/kWh]	0.245	0.28	0.21
Fuel utilization [%]	75	90	60
Recirculation rate [%]	50	85	25
Air temperature increase [%]	150	175	125
ASR (Ωcm^2)	Depends on technology used		
Operating time [Eq. Full Load Hours]	7000		

Table 3
Values used for sensitivity analysis in electrolysis mode.

Modified parameter	Baseline	Best case	Worst case
Stack cost [€/kW]	500	300	700
Selling hydrogen price [€/kg]	4	2	6
Purchase electricity cost[€/kWh]	0.065	0.045	0.085
Steam utilization [%]	75	90	60
Faradaic efficiency [%]	85	95	75
ASR (Ωcm^2)	Depends on technology used		
Operating time [Eq. Full Load Hours]	7000		4380

Table 4
Sensitivity analysis for ammonia production.

Modified parameter	Baseline hydrogen	Baseline water	Best case
Temperature [°C]	400	550	400 550
Pressure [bar]	1	1	20
Faradaic efficiency [%]	2.18 + 42.7	0.33 + 52	88 + 5
Current density [A/cm^2]	0.0395	0.0056	0.319
Faradaic efficiency + Current density	Combination of previous ones		
Faradaic efficiency + Current density + Pressure	Combination of previous ones		

hydrogen production was used to estimate hydrogen costs [5661]. An annual operation and maintenance (O&M) cost of 3.5 % of the total capital investment was assumed. Finally, the economic assessment assumes a system lifetime of 20 years.

3. Results and discussion

In this section, the technical and economic outcomes for all modeled systems are presented. The influence of various operating parameters on system operation and techno-economic performance is investigated. The analysis is conducted in two stages. First, general trends for each operating mode, independent of the cell technology used, are presented. This exploration focuses on the variation of the levelized cost as a function of the change in each operating parameter compared to the baseline condition.

Subsequently, absolute values are provided for each available cell technology, when operating under distinct conditions.

This detailed breakdown allows for a comprehensive understanding of how each technology performs under various operating scenarios as well as providing insight on the best technology.

3.1. Fuel cell operation

The results of the techno-economic study of the two systems in fuel cell mode already introduced are shown in this section.

3.1.1. Economic sensitivity analysis

In this first subsection, the results obtained when only the economic parameters are modified are shown.

3.1.1.1. Stack cost sensitivity analysis. The influence of the stack cost on the plant's overall economics is investigated. Our findings indicate that variations in stack cost, defined in €/kW, primarily affect the total capital expenditure of the plant also influencing the breakdown of CAPEX. When considering the best case scenario, where the lower cost of the stack is considered, with and without electric heaters for the BSCF-BZCY technology, lower overall capital expenses and especially lower contribution of the stack on the overall value are obtained. Stack replacements every five years also exacerbate this effect. This observation can be also highlighted in Fig. 4 where a cost breakdown of the investments required for each component is presented. Finally, a slight

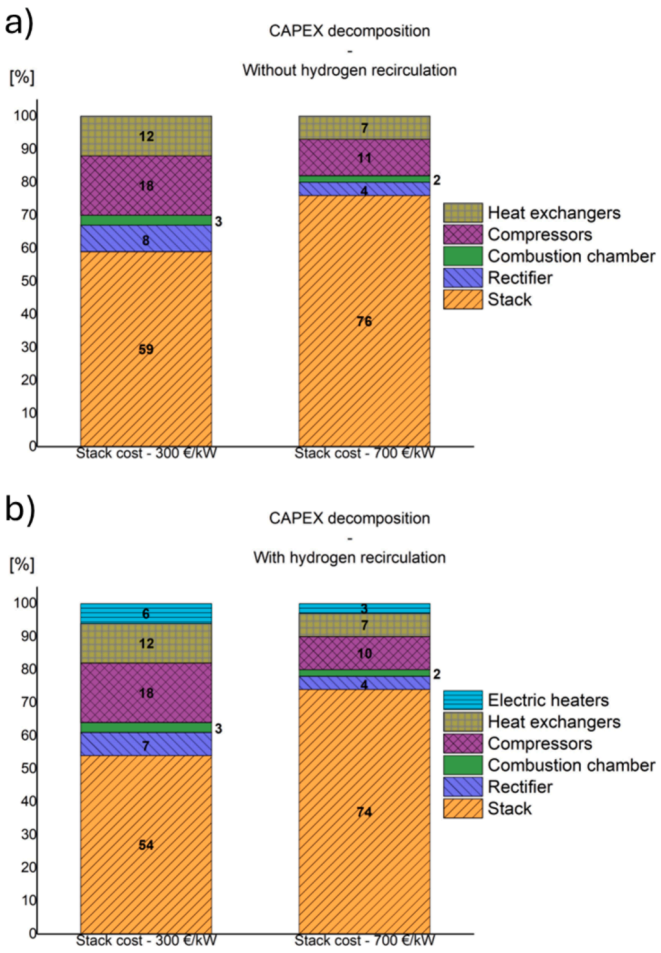

Fig. 4. Stack cost sensitivity analysis FC mode a) without hydrogen recirculation b) with hydrogen recirculation.

impact on the O&M cost, which is linked to the total investment, is observed.

3.1.1.2. Hydrogen cost sensitivity analysis. This analysis reveals an effect only on the operating expenses without affecting the capital expenditures. As Fig. 6 demonstrates, this parameter exhibits one of the highest sensitivities among the parameters considered. Notably, a 45 % increase in the hydrogen cost, compared to the baseline condition, results in a 57 % increase in LCOE. Conversely, the same change in stack cost only leads to a 4 % variation in LCOE.

3.1.1.3. Electricity price sensitivity analysis. This parameter solely affects the overall income, altering the relative contributions of electrical and thermal incomes. By focusing on the cumulative cash flow derived from the sensitivity analysis over 20 years, values for the NPV of 68,000 €, in the best-case scenario, and almost null in baseline conditions, are observed highlighting the substantial influence of this parameter on NPV.

3.1.2. Technical sensitivity analysis

Differently from the first subsection the results obtained when the technical parameters are modified are described.

3.1.2.1. Fuel utilization sensitivity analysis. Parameter considered as the ratio between fuel reacting in the stack and overall flow rate injected, the sensitivity is evaluated by keeping a fixed current density with respect to the baseline one and assuming the cell improvements in the future allow to maintain the same performances therefore neglecting

electrical inefficiencies related to uniform reactions, electrode polarization and mass transfer phenomena [62]. On a system level, increasing fuel utilization leads to a decrease in unreacted hydrogen exiting the stack. Consequently, the combustion chamber (CC) receives less hydrogen as a fuel resulting in the lower temperature of the flue gases with a reduction in the available thermal energy and a decrease of the contribution of the thermal income on the overall one, while keeping the electrical earnings almost constant.

The decrease in the LMTD for the heat exchangers necessitates larger units to maintain heat transfer and increases the cost for these components and their contribution on the CAPEX decomposition of a couple percentual points with going from 4 % to 6 % of the overall expenses. Although the total incomes decrease when higher fuel utilization is reached, the overall economic performances are improved due to lower fuel cost linked with decreased overall hydrogen flow rate injected in the system from $6.79{\cdot}10^{-4} kg/s$ and $4.53{\cdot}10^{-4} kg/s$ respectively in worst and best case for the BSCF-BZCY technology. The sensitivity of the system to fuel utilization can be mitigated by implementing a partial hydrogen recirculation loop redirecting a portion of the unreacted hydrogen back to the stack inlet, with a decrease in the LCOE variation up to 10 percentual points, as highlighted in the comparison between the two systems presented in Fig. 6.

3.1.2.2. Air temperature increase at cathode side sensitivity analysis. Air in the system plays a double role as a reactant and cooling fluid. While passing through the stack, it warms up removing the heat, with a higher amount when the increased operating voltage of the stack is considered, and is associated with the electrochemical reactions, motion of charges, and irreversibility.

Change in the heat exchange effectiveness between the stack and air stream will influence the air temperature increase along the stack. A higher rise in the air temperature between the inlet and outlet of the stack, for example, leads to a reduced air flow rate that must be injected into the system. The main effect of this flow variation is the decrease in the auxiliaries' power consumption to both lower compression power and stream pre-heating consumption with differences respectively of 37 % and 29 % for BSCF-BZCY between the extremes of the range of temperature variations examined in this study. Related to the lower power consumption there is also the decrease in the required size for these components and the corresponding contribution to the CAPEX decomposition. This parameter can be mainly tackled through the optimization of the SRU geometry, especially in terms of interconnectors shape, and is not instead highly related to the MEA contained in it.

3.1.2.3. Stack performances sensitivity analysis. This section explores the impact of variations in a cell's area specific resistance considering the uncertainties in ASR values as reported in the literature and as summarized in Table 1. Additionally, a comparison between different PCFC technologies is included. An increase in ASR means a decrease in the cell performance. This scenario is simulated by maintaining a constant operating current density while changing the ASR. The first key consequence is a lower cell voltage due to higher over potential which has a direct consequence of the change in gross power output with consequent decrease of it. Furthermore, higher ohmic losses within the cell due to increased ASR result in additional heat generation due to irreversibilities. The higher thermal losses reflect into increased cooling air flow rate required with a corresponding rise in the power consumption, size and initial investment from the auxiliary compressors. Potentially, though, increased heat generation translates to a higher heat recovery through the district heating system with a corresponding increase in the contribution that the thermal income has on the overall earnings with a value from 17 % to 28 % when income decomposition between electrical and thermal one is performed. Overall, though, considering both the positive effects on the thermal incomes and the negative on the electrical ones, higher ASR will reflect in worse economic performances. To provide additional numerical values, Fig. 5 presents the absolute changes in key performance parameters for BSCF-BZCY technology when both an increase and decrease of ASR by 20 % are assumed.

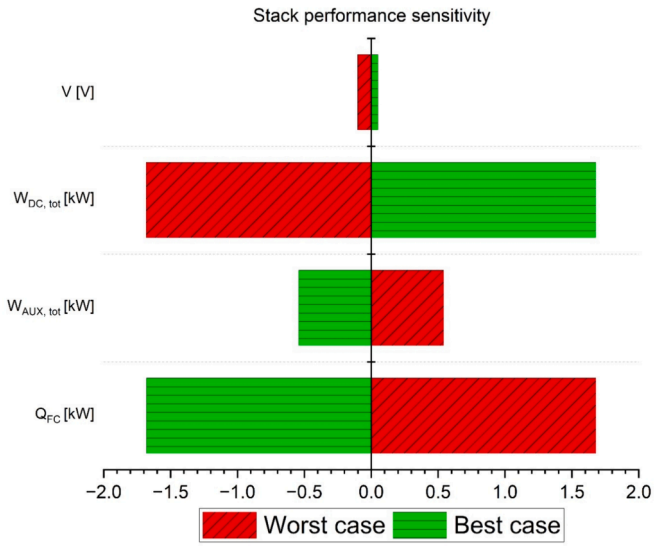

Fig. 5. Variation of FC technical parameters (V operating voltage, $W_{DC,gross}$ overall power, $W_{AUX,tot}$ power required by auxiliary, Q_{FC} waste heat produced) with a 20% ASR change compared to baseline.

3.1.2.4. Recirculation rate sensitivity analysis. This section investigates the impact of varying the recirculation rate (RR) in the second FC system under study. Recirculation involves returning a portion of unreacted hydrogen back to the inlet of the stack from the outlet to reduce the negative effects deriving from the fuel utilization lower than unity. The complexity, and related initial investment, for this system is slightly higher due to the increasing number of components. Increasing the recirculation rate leads first to increased power consumption for the hot fluid compressor, to recover the pressure losses encountered in the stack. Additionally, the recirculated hydrogen is typically warmer than the fresh hydrogen entering the system and, by blending them, the temperature of the mixed hydrogen stream entering the pre-heater increases consequently requiring less heat for it to reach the target temperature and therefore lowering the auxiliary heater consumption. While recirculation offers benefits in the reduction of heater consumption, it also has drawbacks as a reduction in the amount of hydrogen entering the combustion chamber which translates to less available hydrogen for fuel, leading to a decrease in recoverable thermal energy. This, in turn, lowers both thermal and overall system incomes. However, the decrease in fuel consumption due to higher hydrogen utilization, with a decrease in hydrogen flow rate at the inlet of the system equal to 16 %, between the two extremal operating values can outweigh the reduction of thermal income which is only of 7 %. Overall beneficial effects from a higher recirculation can be highlighted.

3.1.3. Sensitivity comparison in fuel cell mode

A graphical comparison of all the sensitivity analyses performed, both with and without hydrogen recirculation, is hereafter shown in Fig. 6. The exploitation of this figure allows to evaluate how small changes in key parameters affect the overall outcomes, especially in the economic assessment. By comparing the sensitivity of the LCOE to the different parameters examined in fuel cell mode, the purchase hydrogen cost is the one with the highest sensitivity especially when compared to other variations such as the one related to the stack cost which has a sensitivity almost 10 times lower. With an additional focus on the technical parameters, the ASR showed the highest sensitivity followed by fuel utilization and an increase of the air temperature when flowing

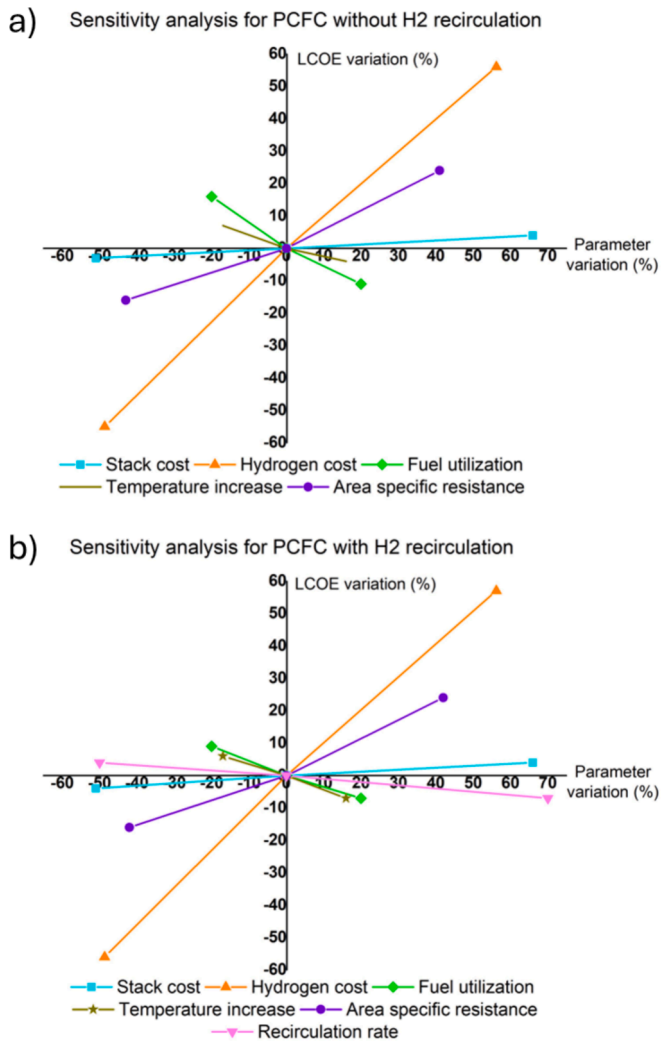

Fig. 6. LCOE variation from baseline condition from sensitivity analysis in FC mode a) without hydrogen recirculation b) with hydrogen recirculation.

through the stack. As already noted, the sensitivity to the fuel utilization can be reduced when partial recirculation of the unreacted hydrogen is performed as shown when comparing Fig. 6a and Fig. 6b.

Numerical values for the LCOE with baseline, best, and worst overall operating parameters are summarized in Table 5. Operating conditions for the best and worst case are defined by considering, all at the same time, the values for the FU, recirculation rate, air temperature increase, and ASR defined respectively in columns 2 and 3 of Table 2.

As highlighted from these results, stack based on a technology that exploits LSCF material as electrode materials presents better performances in all examined scenarios as shown by comparing BSCF-BZCY and LSCF-BZCY values in Table 5. Similar observation can also be extrapolated in terms of electrolyte materials with BZCYYb having better performances than BZCY as highlighted by a comparison between LSCF-BZCY and LSCF-BZCYYb technologies comparison.

Table 5
Levelized cost of electricity in comparison with different technologies.

	BSCF-BZCY [17 stacks of 100 cells]	LSCF-BZCY [16 stacks of 100 cells]	LSCF- BZCYYb [15 stacks of 100 cells]
Baseline	0.248 €/kWh	0.238 €/kWh	0.214 €/kWh
	0.258 €/kWh	0.248 €/kWh	0.223 €/kWh
Worst case	0.395 €/kWh	0.337 €/kWh	0.296 €/kWh
overall	0.407 €/kWh	0.352 €/kWh	0.308 €/kWh
Best case over-	0.200 €/kWh	0.195 €/kWh	0.183 €/kWh
all	0.199 €/kWh	0.194 €/kWh	0.182 €/kWh
Best case over-	0.233 €/kWh	0.208 €/kWh	0.213 €/kWh
all for 4380 h	0.228 €/kWh	0.224 €/kWh	0.209 €/kWh

For both comparisons, this conclusion can be explained by the different ASR values. It is also important to highlight that LSCF and BZCYYb are used as precursors in the manufacturing process especially for powder synthesis, materials, such as ytterbium oxides, with a cost higher than the yttrium oxides which are substituted with a corresponding increase in the expected cost of the cells. At the same time, it should also be considered that the introduction of ytterbium in the perovskite has been found to exhibit higher densification and lower grain size compared to BZCY in the same sintering conditions which may help during the sintering process of the cell manufacturing step [12]. This final aspect is critical also to improve the scalability of this technology making ideally the manufacturing process easier and faster.

Therefore, especially considering the highest sensitivity of the LCOE associated with the operation phase, with the more marginal contribution of the capital expenses correlated to the stack, it can be concluded that the LSCF-BZCYYb is a better choice since the higher expected cost that may derive from the use of ytterbium may be overcome by the higher efficiencies and performances of the cells.

Regarding the comparison between the two systems, without or with partial recirculation of the unreacted hydrogen, the second solution presents overall the best performance especially due to the lower expenses linked to lower hydrogen consumption. This system is also expected to have a higher flexibility, for example by modifying the recirculation rate, to tune the electricity and thermal ratios produced by the system with the requirements, and to better adapt to the energy trends from a technical and economic point of view.

3.2. Electrolysis operation

The results for the single system working in electrolysis mode are described in this section.

3.2.1. Economic sensitivity analysis

In this first subsection, the results from economic aspects sensitivity are shown.

3.2.1.1. Stack cost sensitivity analysis. Fig. 7 shows results similar to the fuel cell ones shown in Fig. 4 with higher expenses reached in the worst case, when higher stack costs are used, when also higher contribution of the stack compared to the other BoP elements is observed. No further insights are presented compared to the prior case except for a slightly higher sensitivity especially linked to the higher power of the stack in electrolysis mode.

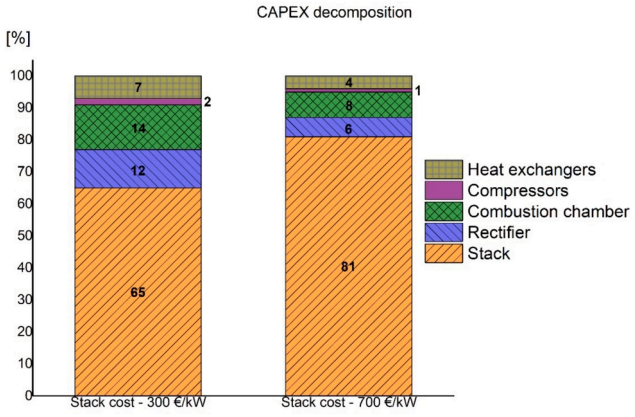

Fig. 7. Stack cost sensitivity analysis EC mode in worst and best case scenarios.

3.2.1.2. Electricity cost sensitivity analysis. Like the previous section, electricity cost determines a significant sensitivity over the levelized cost of hydrogen, compared to other economic factors. A 40 % increase in electricity cost relative to baseline condition translates to a 30 % rise in LCOH. In contrast, the same change to the stack cost leads to a 5 % variation in LCOH. For BSCF-BZCY technology, this translates into an increase in the LCOH from 3.13 €/kg to 4.97 €/kg with unchanged operating hours further highlighting the higher impact of the operating phase on the final cost of hydrogen with respect to the one related to the initial investment.

3.2.2. Technical sensitivity analysis

In this second section, the results obtained when technical parameter sensitivity is performed are highlighted.

3.2.2.1. Steam utilization sensitivity analysis. This section explores the impact of varying the steam utilization (SU), defined as the percentage of steam reacting compared to the total steam flow entering the stack. The analysis is conducted while maintaining a constant hydrogen production rate. Increasing the SU, while assuming cells can maintain the performances defined by the ASR, leads to consequences on system performance. First, a lower water flow rate, up to four times less in the best case compared to the worst case scenario, will have to be injected, and also pre-heated, vaporized, and superheated, which will decrease the auxiliary heater consumption, and initial investments, while increasing the electrical efficiency because as stated the output hydrogen is considered as constant. The increased SU alters the system's flow rates, due to a decrease in the amount of unreacted water exiting the stack, and therefore a lower amount of heat available for recovery within the system, all this also affecting the layout of the internal heat exchangers. This last variation will also decrease thermal incomes, by approximately 5 %, while improving heat management and utilization.

3.2.2.2. Faradaic efficiency sensitivity analysis. This section investigates the impact of variations in Faradaic efficiency on the system's performance and the analysis is conducted maintaining constant current density. An increase in the faradaic efficiency translates to a greater amount of hydrogen produced for a given amount of electrical current and input, raising the hydrogen flow rate exiting the stack, but this also produces a slight increase in the power required for the hydrogen circulation. The additional water required to achieve higher hydrogen production, defined by stoichiometry, will also increase the overall auxiliary components' energy consumption and size. Despite these higher consumptions, the overall efficiencies and incomes will increase, determining a decrease in the LCOH and advantageous economic performances.

3.2.2.3. Stack performances sensitivity analysis. This section examines the impact of variations in a cell's area specific resistance on the performance of the stack while maintaining a thermoneutral condition. An increase in the ASR will principally result in a lower current density due to the higher over-potentials with an associated decrease in the overall amount of hydrogen produced by the stack and related incomes. With reduced hydrogen production, the system requires a lower steam flow rate, because it is evaluated with stoichiometry with respect to the output hydrogen. The lower water request translates into a beneficial decrease in auxiliary electric power for water vaporization. The effects of ASR change in terms of auxiliary power, hydrogen flow rate, and current density are highlighted in Fig. 8.

3.2.3. Sensitivity comparison in electrolysis mode

A graphical comparison of all the sensitivity analyses performed is hereafter shown in Fig. 9. From the comparison of the LCOH variation to the different parameters examined, electricity purchase price and faradaic efficiency present the highest sensitivities almost comparable with each other. Steam utilization and area specific resistance are the following parameters with sensitivities fivefold smaller sensitivities.

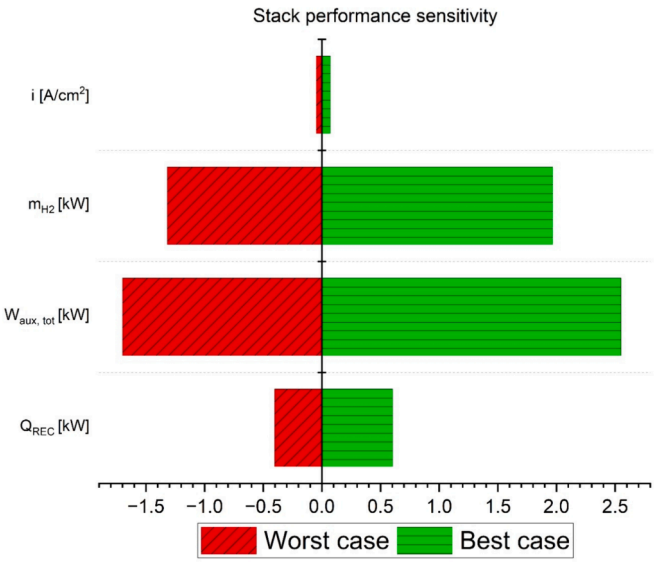

Fig. 8. Variation of EL technical parameters (i current density, m_{H2} hydrogen flow rate, $W_{AUX,tot}$ power required by auxiliary, Q_{REC} heat recovered) with a 20% ASR change compared to baseline.

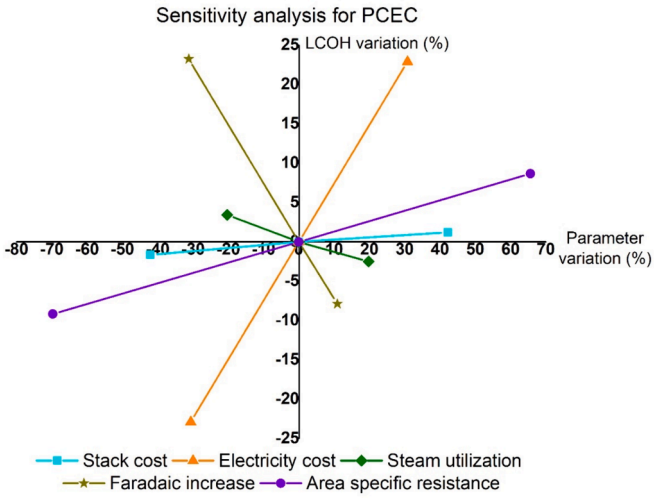

Fig. 9. LCOH variation from baseline condition from sensitivity analysis in EC mode.

Numerical values for the LCOH with baseline, best, and worst overall operating parameters, taking into account different operating hours and

Table 6
Levelized cost of hydrogen in comparison with different technologies.

	BSCF-BZCY [12 stacks of 100 cells]	LSCF-BZCY [12 stacks of 100 cells]	LSCF-BZCYYb [7 stacks of 100 cells]	Current technology
Baseline	4.57	4.57	4.56	3.8 – 4.9
Worst case overall	5.23	5.23	5.22	
Best case overall	4.01	4.01	3.97	
Best case overall for 4380 h	4.81	4.81	4.80	

also in comparison to the current high temperature technologies available when using electricity with a similar cost, are summarized in Table 6.

Conclusions similar to the fuel cell systems can be extrapolated from the results presented in Table 6, showing LSCF and BZCYYb respectively as the best electrode and electrolyte materials with the corresponding characteristics linked to the manufacturing process. Again, the highest sensitivity is related to the operation phase, and therefore, the idea of increasing the initial cost to reach higher performances and better operations would be reasonable.

It should be noted that despite LSCF-BZCYYb technology being the best overall, results are close to each other because each system is assumed to operate in thermoneutral conditions. If the systems are operated with a constant current density approach, instead, the divergence between the different technologies will increase in favor of the LSCF-BZCYYb ones. It is important to highlight how, if proper performances are kept during scale up, an LCOH comparable to or better than the current technologies can be reached showing the competitiveness of this solution.

3.3. Ammonia synthesis

The technical and economic performance of both systems are evaluated, performing a sensitivity analysis with the parameters introduced in Table 4. While upstream hydrogen production simplifies ammonia electrocatalysis, it might decrease economic viability due to double energy consumption through separate stacks. Both configurations exhibit complex subsystems composition, as ASU, electrolysis, liquefaction system, and purification unit, providing complex results already in baseline conditions.

3.3.1. Operating pressure sensitivity analysis

This section investigates the effect of increasing the operating pressure from 1 to 20 bar. This shifts the thermodynamic equilibrium towards the ammonia with yield variations, of approximately 10 times compared to baseline, as available from internal knowledge in the EIFER research center. The favored ammonia production rate will increase the income from ammonia, contributing positively to the overall earnings, and improve the heat recovered during ammonia condensation with corresponding higher thermal income. At the same time, the pressurized system experiences a decrease in the Nernst potential for the upstream electrolyzer as well as requiring more energy for the auxiliaries due to the compression of the streams required. Higher operating pressure should improve the performances at higher current densities, but this effect is neglected to keep conservative scenarios.

Finally, also an increase in the contribution of the ASU, for both CAPEX and OPEX, due to a higher nitrogen conversion ratio and higher reintroduced reactant can be highlighted.

Despite the benefit of higher ammonia production, the system modification remains unfavorable because the income gains are outweighed by the increased energy consumption associated with the pressurization of the streams involved in the system and especially of the ones injected into the system.

3.3.2. Faradaic efficiency sensitivity analysis

This section explores the effect of varying faradaic efficiencies for ammonia and hydrogen production. The values are selected to achieve collective efficiency close to 93 % given by the combination of 88 % for the ammonia and 5 % for the hydrogen, an unwanted byproduct in this case study. It can be highlighted how this variation improved both overall conversion and selectivity of the output products. This would be especially reached with specific catalyst that may differ from those considered in this work.

An increase in the faradaic efficiency, assuming a current density constant to the baseline condition, will increase the ammonia production, and its contribution to the overall income, decreasing at the same time the hydrogen output and related earnings. In addition, higher thermal incomes, due to an increase in the energy recovered from the ammonia liquefaction, are observed. This increase is especially linked with the condensation phase. Similarly to the previous subsection, the nitrogen used, and therefore freshly separated from the air, will increase, also raising the ASU contribution to both initial investment and operative costs.

3.3.3. Current density sensitivity analysis

Current density variation, performed keeping thermo-neutral, is performed with an increase up to 0.319 A/cm^2 similar to values of FC and EL mode. By doing so a slight increase in the ammonia production and a strongly higher productivity of hydrogen, in terms of absolute values, are observed due to the different faradaic efficiencies for the two products which are maintained as favorable to hydrogen production. From a relative point of view, though, the increase of flow rates is almost linear with the current density and therefore is equal, in this study, to eight times. Again, the contribution of the air separation unit is slightly increased just due to the slightly increase of ammonia production and connected nitrogen usage. The rising stack power consumption, and the corresponding electrical expenses, remains what affects the technical and economic performances of this case study making this solution unreasonable.

3.3.4. Current density and faradaic efficiency sensitivity analysis

Considering the disadvantageous outcome of simple current density increase, the combination of this upgrade with the increase of faradaic efficiency is also investigated. By doing so, in combination with the higher energy consumption and increase in the overall expenses, also an increase in the output products and related incomes can be observed. A strong increase of ammonia, close to 300 times, is observed, while the hydrogen remains almost constant due to a trade-off between higher current density and lower faradaic efficiency. The cost for the ASU investment and operation is also strongly increased due to higher nitrogen consumed according to stoichiometry. Overall, this is the first economically advantageous case study observed and is considered as the most convenient solution as highlighted in Fig. 10.

3.3.5. Current density, faradaic efficiency, and pressure sensitivity analysis

In this section, both electrochemical improvements, linked to the current density and faradaic efficiency, and thermodynamic, obtained from the higher pressure, are simulated reaching results more reasonable because obtained by acting on two different types of improvements. By these variations a strong increase in ammonia production, again close to 300 times, and linked earnings, as well as constant hydrogen can be

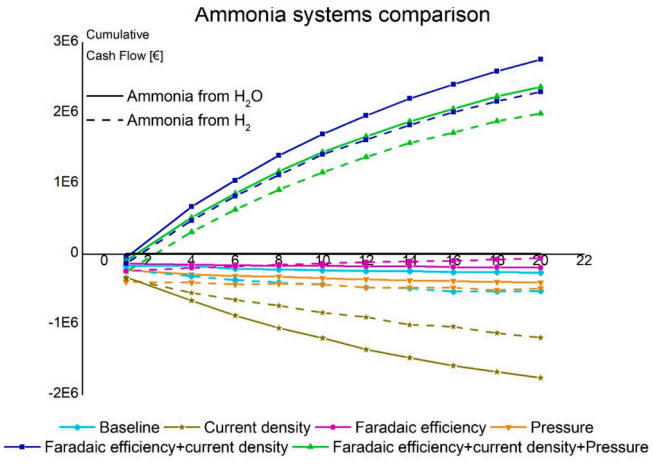

Fig. 10. Comparison of cumulative cash flows for different ammonia production systems.

Table 7
LCOA comparison of different systems and technologies.

	Ammonia production H_2		Ammonia production H_2O		Current ammonia produced via green hydrogen	Current ammonia produced via the Haber-Bosch process
LCOA [€/kgNH_3]	1.21	0.995	0.782	0.664	0.790 – 0.962	0.300 – 0.600
Capacity [ton/year]	150	1000	150	1000	Not specified	

observed. In combination with the higher incomes also higher energy consumption, complexity and initial investment of the plant, with an auxiliary power increase of a few tents, depending on the flow rate, is obtained. This occurs due to two contributions, one linked to the stack operation and another with the required stream pressurization.

Higher ASU contribution is observed while variation in uphill stack production capability is neglected. This case study is also economically advantageous with lower LCOA compared to the examples introduced in the previous section as highlighted in Fig. 10.

3.3.6. *Ammonia synthesis technology comparison*

A comparison between the two different technologies studied is hereafter provided by showing cumulative cash flow and LCOA also according to variable production capacity. The difference in cumulative cash flows, considering electricity cost of 0.065 €/kWh, DH injection price of 0.06 €/kWh, ammonia price of 2.4 €/kg, and Hydrogen cost of 3.9 €/kg, are shown in Fig. 10.

A comparison of the LCOA for the produced green ammonia, also with respect to the current green ammonia and conventional route [56,64], is summarized in Table 7.

From these values the advantage of direct water injection, if the same electrochemical performances as the hydrogen injection system are reached and especially if the size of the plant is increased, by connecting a higher number of stacks and proper power control, can be highlighted. This last aspect also goes in parallel with the current trend linked to the scale up of the electrolysis plant up to GW scale [63]. As already stated, the expenses related to the material costs and manufacturing are expected to be higher with direct water splitting due to the expected catalysts required to reach an economically sustainable ammonia production rate. A detailed cost decomposition of the stack elements has not been performed here, but it could be a useful topic for future research. Still, due to the high sensitivity of the operation phase, more expensive systems with strongly higher performances would still be beneficial.

The product, by looking at the price, would also be competitive with the current green ammonia produced, but a further reduction would still be required to compete with the traditional Haber-Bosch process. Additional improvements, which would make the system more competitive, would derive from the increase in the nitrogen conversion ratio inside of the stack with respect to the 65 % assumed. The increase of this parameter would decrease the flow rate of all the streams strongly decreasing the energy consumption related to the auxiliaries of the system.

4. Conclusions and Outlook

In conclusion, the PCCs technology can reach competitive performances in the different applications explained especially in terms of electrical efficiencies and energy consumption. This is valid from both the technical and economic point of view already by taking into account intermediate performances among those available in the literature.

This is possible if the development of the technology allows it to reach good performances and scale up, especially if standardized materials are defined which would also help its commercialization.

Critical aspects to focus on, according also to the outcomes of this analysis, are the following:

1. Manufacturing: improved sinterability of the layers especially for electrolyte materials which would simplify the manufacturing process, decreasing the maximum temperature or time required. Furthermore, also an increase in the grain size at the end of the process would improve the conductivity.
2. General operation: improve the conductivity, reducing the ASR to improve the overall performances in terms of efficiency during both fuel cell and electrolysis mode. Ideally, this increase should also be performed guaranteeing stability for long term operation.
3. Electrolysis operation: improve steam utilization, in order to reduce the consumption especially related to the auxiliaries for water evaporation. Improve the faradaic efficiency being it the most important parameter during the operation and that would therefore decrease the most the hydrogen cost.
4. Fuel cell operation; act on the fuel utilization as the main parameter. If this improvement is not managed by the research sector, the exploitation of a recirculation of unreacted hydrogen into the system would improve the performances
5. Ammonia synthesis: cell with structural properties able to withstand high-pressure operation, which would increase the ammonia yield due to thermodynamics. The most impactful and important and critical parameters to improve would be current density and faradaic efficiency until reaching a flow rate of approximately of $10^{-8}\frac{mol}{cm^2 s}$ to $10^{-7}\frac{mol}{cm^2 s}$ which would make the system economically sustainable

Overall, considering the tradeoff between the advantages and disadvantages of these PCCs compared to the commercial ones, its competitiveness is evidenced if proper development and scale up of the technology, which allows maintaining structural integrity and unchanged electrochemical performances, are reached also to reduce the stack investment cost. Still, it should be noted that this research finds some limitations especially when addressing the uncertainty, especially on economic assumptions, which would affect the economic viability of this technology.

The importance of the operation phase, especially with respect to the initial investment, is highlighted in this study. For future developments, the criticality in obtaining cells with better performances, which for each application would be obtained by following the conclusions defined in the final numbered list provided, even if higher initial costs would be reached for example through the exploitation of BZCYYb as electrolyte material is highlighted.

To finalize these scale up and improvements, policymakers should support research and development through funding and policies also between different research institutions and industry to reach common outcomes. Engineers and researchers should act of manufacturability, scalability and operational efficiency also in terms of BoP optimization, while exploring advanced materials or cell architectures.

CRediT authorship contribution statement

Andrea Moranti: Writing – review & editing, Writing – original draft, Visualization, Validation, Software, Resources, Methodology, Investigation, Formal analysis, Data curation, Conceptualization. **Julian Dailly:** Writing – review & editing, Visualization, Validation, Supervision, Resources, Project administration, Methodology, Investigation, Data curation, Conceptualization. **Massimo Santarelli:** Writing – review & editing, Visualization, Validation, Supervision, Resources,

Methodology, Investigation, Data curation, Conceptualization. **Federico Smeacetto:** Writing – review & editing, Visualization, Validation, Supervision, Resources, Project administration, Methodology, Investigation, Data curation.

Declaration of competing interest

The authors declare that they have no known competing financial interests or personal relationships that could have appeared to influence the work reported in this paper.

Data availability

Data will be made available on request.

Acknowledgment

The authors acknowledge the collaborations carried out between the European Institute for Energy Research (EIFER) and the Politecnico di Torino that made this work possible.

References

[1] Yolcan OO. World energy outlook and state of renewable energy: 10-Year evaluation. Innov Green Developm 2023;2(4):100070. https://doi.org/10.1016/j.igd.2023.100070.
[2] Lagadec MF, Grimaud A. Water electrolysers with closed and open electrochemical systems. Nat Mater 2020;19(11):1140–50. https://doi.org/10.1038/s41563-020-0788-3.
[3] Dubois A, Ricote S, Braun RJ. Benchmarking the expected stack manufacturing cost of next generation, intermediate-temperature protonic ceramic fuel cells with solid oxide fuel cell technology. J Power Sources 2017;369:65–77. https://doi.org/10.1016/j.jpowsour.2017.09.024.
[4] Duan C, et al. Highly efficient reversible protonic ceramic electrochemical cells for power generation and fuel production. Nat Energy 2019;4(3):230–40. https://doi.org/10.1038/s41560-019-0333-2.
[5] Ferrero D, Lanzini A, Santarelli M, Leone P. A comparative assessment on hydrogen production from low- and high-temperature electrolysis. Int J Hydrogen Energy 2013;38(9):3523–36. https://doi.org/10.1016/j.ijhydene.2013.01.065.
[6] Bello IT, et al. Materials development and prospective for protonic ceramic fuel cells. Int J Energy Res 2022;46(3):2212–40. https://doi.org/10.1002/er.7371.
[7] Mendes SR, da Silva GMG, Araújo ES, Faia PM. A review on low-temperature protonic conductors: principles and chemical sensing applications, 01. Multidisciplinary Digital Publishing Institute (MDPI; Jun. p. 2024). https://doi.org/10.3390/chemosensors12060096.
[8] Cheng S, Li X, Huang X, Ling Y, Liu S, Li T. Hydrogen separation via proton conducting ceramic membranes: a review. Int J Hydrogen Energy 2024;70:654–65. https://doi.org/10.1016/j.ijhydene.2024.05.181.
[9] Kyriakou V, et al. Methane steam reforming at low temperatures in a BaZr0.7Ce0.2Y0.1O2.9 proton conducting membrane reactor. Appl Catal B 2016;186:1–9. https://doi.org/10.1016/j.apcatb.2015.12.039.
[10] Lee J, Otomo J. Proton conduction-assisted direct CO2 methanation using Ni/CaO/Y-doped BaZrO3 proton conductor. Fuel 2022;322:124094. https://doi.org/10.1016/j.fuel.2022.124094.
[11] Wang B, Li T, Gong F, Othman MHD, Xiao R. Ammonia as a green energy carrier: electrochemical synthesis and direct ammonia fuel cell - a comprehensive review. Fuel Process Technol 2022;235:107380. https://doi.org/10.1016/j.fuproc.2022.107380.
[12] Danilov NA, Starostina IA, Starostin GN, Kasyanova AV, Medvedev DA, Shao Z. Fundamental understanding and applications of protonic Y- and Yb-Coped Ba(Ce,Zr)O3 perovskites: state-of-the-art and perspectives. Adv Energy Mater 2023;13(47):2302175. https://doi.org/10.1002/aenm.202302175.
[13] Le LQ, et al. Proton-conducting ceramic fuel cells: Scale up and stack integration. J Power Sources 2021;482:228868. https://doi.org/10.1016/j.jpowsour.2020.228868.
[14] Vignesh D, Rout E. Technological challenges and advancement in proton conductors: a review. Energy Fuel Mar. 2023;37(5):3428–69. https://doi.org/10.1021/acs.energyfuels.2c03926.
[15] Lin B, et al. Intermediate-to-low temperature protonic ceramic membrane fuel cells with Ba0.5Sr0.5Co0.8Fe0.2O3-δ–BaZr0.1Ce0.7Y0.2O3-δ composite cathode. J Power Sources 2009;186(1):58–61. https://doi.org/10.1016/j.jpowsour.2008.09.041.
[16] Marrony M, Dailly J. Advanced proton conducting ceramic cell as energy storage device. J Electrochem Soc 2017;164:F988–94. https://doi.org/10.1149/2.1541709jes.
[17] Yoo Y, Lim N. Performance and stability of proton conducting solid oxide fuel cells based on yttrium-doped barium cerate-zirconate thin-film electrolyte. J Power Sources 2013;229:48–57. https://doi.org/10.1016/j.jpowsour.2012.11.094.
[18] Dailly J, Ancelin M, Marrony M. Long term testing of BCZY-based protonic ceramic fuel cell PCFC: Micro-generation profile and reversible production of hydrogen and electricity. Solid State Ion 2017;306:69–75. https://doi.org/10.1016/j.ssi.2017.03.002.
[19] Xie Y, et al. La-doped Ba0.5Sr0.5Co0.8Fe0.2O3−δ air electrodes with enhanced performance and stability for reversible protonic ceramic cells. J Electrochem Soc 2023;170(2):24513. https://doi.org/10.1149/1945-7111/acbb2f.
[20] Bi L, Fabbri E, Traversa E. Novel Ba0.5Sr0.5(Co0.8Fe0.2)1 − xTixO3 − δ (x = 0, 0.05, and 0.1) cathode materials for proton-conducting solid oxide fuel cells. Solid State Ion 2012;214:1–5. https://doi.org/10.1016/J.SSI.2012.02.049.
[21] Yan D, et al. Multi-physical and electrochemical coupling model for the protonic ceramic fuel cells with H+/e−/O2− mixed conducting cathodes. Appl Sci 2022;12(8):pp. https://doi.org/10.3390/app12083889.
[22] Lee K-R, et al. Fabrication of anode-supported thin BCZY electrolyte protonic fuel cells using NiO sintering aid. Int J Hydrogen Energy 2019;44(42):23784–92. https://doi.org/10.1016/j.ijhydene.2019.07.097.
[23] Lee S, Park S, Wee S, woo Baek H, Shin D. One-dimensional structured La0.6Sr0.4Co0.2Fe0.8O3−δ - BaCe0.5Zr0.35Y0.15O3−δ composite cathode for protonic ceramic fuel cells. Solid State Ion 2018;320:347–52. https://doi.org/10.1016/j.ssi.2018.03.010.
[24] Lee H, Lee S, Lee T, Park S, Shin D. Long term stability of porosity gradient composite cathode controlled by electro-static slurry spray deposition. Int J Hydrogen Energy 2017;42(6):3748–52. https://doi.org/10.1016/j.ijhydene.2016.09.077.
[25] Yang L, Liu Z, Wang S, Choi Y, Zuo C, Liu M. A mixed proton, oxygen ion, and electron conducting cathode for SOFCs based on oxide proton conductors. J Power Sources 2010;195(2):471–4. https://doi.org/10.1016/j.jpowsour.2009.07.057.
[26] Nguyen NTQ, Yoon HH. Preparation and evaluation of BaZr0.1Ce0.7Y0.1Yb0.1O3−δ (BZCYYb) electrolyte and BZCYYb-based solid oxide fuel cells. J Power Sources 2013;231:213–8. https://doi.org/10.1016/j.jpowsour.2013.01.011.
[27] Zhang Q, Hou Y, Chen L, Wang L, Chou K. Enhancement of electrochemical performance for proton conductive solid oxide fuel cell by 30%GDC-LSCF cathode. Ceram Int 2022;48(12):17816–27. https://doi.org/10.1016/j.ceramint.2022.03.052.
[28] Chen X, et al. [LSCF-BZCYYb3] Fabrication and performance of anode-supported proton conducting solid oxide fuel cells based on BaZr0.1Ce0.7Y0.1Yb0.1O3-δ electrolyte by multi-layer aqueous-based co-tape casting. J Power Sources 2021;506:229922. https://doi.org/10.1016/j.jpowsour.2021.229922.
[29] Shimada H, Yamaguchi Y, Sumi H, Mizutani Y. Performance comparison of perovskite composite cathodes with BaZr0.1Ce0.7Y0.1Yb0.1O3–δ in anode-supported protonic ceramic fuel cells. J Electrochem Soc 2020;167(12):124506. https://doi.org/10.1149/1945-7111/abab26.
[30] Niu Y, et al. Highly active and durable air electrodes for reversible protonic ceramic electrochemical cells enabled by an efficient bifunctional catalyst. Adv Energy Mater 2022;12(12):2103783. https://doi.org/10.1002/aenm.202103783.
[31] Zhou Y, et al. An efficient bifunctional air electrode for reversible protonic ceramic electrochemical cells. Adv Funct Mater 2021;31(40):2105386. https://doi.org/10.1002/adfm.202105386.
[32] Klinsrisuk S, Irvine JTS. Electrocatalytic ammonia synthesis via a proton conducting oxide cell with BaCe0.5Zr0.3Y0.16Zn0.04O3-δ electrolyte membrane. Catal Today 2017;286:41–50. https://doi.org/10.1016/j.cattod.2016.06.051.
[33] Yun DS, Joo JH, Yu JH, Yoon HC, Kim JN, Yoo CY. Electrochemical ammonia synthesis from steam and nitrogen using proton conducting yttrium doped barium zirconate electrolyte with silver, platinum, and lanthanum strontium cobalt ferrite electrocatalyst. J Power Sources 2015;284:245–51. https://doi.org/10.1016/j.jpowsour.2015.03.002.
[34] Pirou S, et al. Planar proton-conducting ceramic cells for hydrogen extraction: mechanical properties, electrochemical performance and up-scaling. Int J Hydrogen Energy 2022;47(10):6745–54. https://doi.org/10.1016/j.ijhydene.2021.12.041.
[35] Braun RJ, et al. Development of kW-Scale protonic ceramic fuel cells and systems. ECS Trans Jul. 2019;91(1):997. https://doi.org/10.1149/09101.0997ecst.
[36] Ferguson K, Dubois A, Albrecht K, Braun RJ. [PCFC BOP]High performance protonic ceramic fuel cell systems for distributed power generation. Energy Convers Manag 2021;248:114763. https://doi.org/10.1016/j.enconman.2021.114763.
[37] Kee RJ, Ricote S, Zhu H, Braun RJ, Carins G, Persky JE. [SOEC_inlet T steam] perspectives on technical challenges and scaling considerations for tubular protonic-ceramic electrolysis cells and stacks. J Electrochem Soc 2022;169(5):54525. https://doi.org/10.1149/1945-7111/ac6c4e.
[38] Morgan ER, McGowan JG, "Techno-economic feasibility study of ammonia plants powered by offshore wind," United States – Massachusetts, 2013. [Online]. Available: https://www.proquest.com/dissertations-theses/techno-economic-feasibility-study-ammonia-plants/docview/1323774328/se-2?accountid=28840.
[39] Elcogen, "Solid oxide stacks for fuel cell systems; Affordable Green Hydrogen," Jun. 2024. [Online]. Available: https://elcogen.com/products/solid-oxide-stacks-for-fuel-cell-systems/.
[40] Shimoda N, Kobayashi Y, Kimura Y, Nakagawa G, Satokawa S. Electrochemical synthesis of ammonia using a proton conducting solid electrolyte and nickel cermet electrode. J Ceram Soc Jpn 2017;125(4):252–6. https://doi.org/10.2109/jcersj2.16286.
[41] Bucsa S, et al. Exergetic analysis of a cryogenic air separation unit. Entropy 2022;24(2). https://doi.org/10.3390/e24020272.
[42] Lin L, Tian Y, Su W, Luo Y, Chen C, Jiang L. Techno-economic analysis and comprehensive optimization of an on-site hydrogen refuelling station system using

ammonia: hybrid hydrogen purification with both high H2 purity and high recovery. Sustain Energy Fuels 2020;4(6):3006–17. https://doi.org/10.1039/C9SE01111K.
[43] "The NIST Chemistry Webbook | NIST," Mar. 2018. [Online]. Available: https://www.nist.gov/programs-projects/nist-chemistry-webbook.
[44] "Compressibility Factor from Redlick-Kwong Equations.".
[45] Turton R, Bailie RC, Whiting WB, Shaeiwitz JA, Bhattacharyya D, "Analysis, Synthesis, and Design of Chemical Processes Fourth Edition.".
[46] C. Engineering, "Plant Cost Index," Aug. 2024. [Online]. Available: https://www.chemengonline.com/site/plant-cost-index/.
[47] Dimian AC, Bildea CS. Appendix B: Heat-Exchanger Design," in *Chemical Process D*. Wiley; 2008. p. 474–82. https://doi.org/10.1002/9783527621583.app2.
[48] Jamshidi M, Askarzadeh A. Techno-economic analysis and size optimization of an off-grid hybrid photovoltaic, fuel cell and diesel generator system. Sustain Cities Soc 2019;44:310–20. https://doi.org/10.1016/j.scs.2018.10.021.
[49] Fraunhofer ISE, "Study: Current and Future cost of Photovoltaics," 2015. [Online]. Available: https://www.ise.fraunhofer.de/en/publications/studies/studie-current-and-future-cost-of-photovoltaics-long-term-scenarios-for-market-development-system-prices-and-lcoe-of-utility-scale-pv-systems.html.
[50] Sangwongwanich A, Yang Y, Sera D, Blaabjerg F, Zhou D. On the impacts of PV array sizing on the inverter reliability and lifetime. IEEE Trans Ind Appl 2018;54(4):3656–67. https://doi.org/10.1109/TIA.2018.2825955.
[51] Theis J. Quality guidelines for energy systems studies: cost estimation methodology for NETL assessments of power plant performance. United States 2021. https://doi.org/10.2172/1567736.
[52] Ebrahimi A, Ziabasharhagh M. Optimal design and integration of a cryogenic Air Separation Unit (ASU) with Liquefied Natural Gas (LNG) as heat sink, thermodynamic and economic analyses. Energy 2017;126:868–85. https://doi.org/10.1016/j.energy.2017.02.145.
[53] Fu C, Gundersen T. [ASU specific energy consumption] Using exergy analysis to reduce power consumption in air separation units for oxy-combustion processes. Energy 2012;44(1):60–8. https://doi.org/10.1016/j.energy.2012.01.065.
[54] Bui T, Lee D, Ahn KY, Kim YS. Techno-economic analysis of high-power solid oxide electrolysis cell system. Energy Convers Manag 2023;278:116704. https://doi.org/10.1016/j.enconman.2023.116704.
[55] Wang J, Al-attab KA, Yew Heng T. Techno-economic and thermodynamic analysis of solid oxide fuel cell combined heat and power integrated with biomass gasification and solar assisted carbon capture and energy utilization system. Energy Convers Manag 2023;280:116762. https://doi.org/10.1016/j.enconman.2023.116762.
[56] Devkota S, Ban S, Shrestha R, Uprety B. Techno-economic analysis of hydropower based green ammonia plant for urea production in Nepal [green ammonia and hydrogen price]. Int J Hydrogen Energy 2023;48(58):21933–45. https://doi.org/10.1016/j.ijhydene.2023.03.087.
[57] Singla R, Chowdhury K. [ASU consumption (0,4 kWh/kgO2)] Mitigating an increase of specific power consumption in a cryogenic air separation unit at reduced oxygen production. IOP Conf Ser Mater Sci Eng 2017;171(1):12016. https://doi.org/10.1088/1757-899X/171/1/012016.
[58] E. Engineeringtoolbox, "Critical Temperatures and Pressures for some Common Substances," Mar. 2023. [Online]. Available: https://www.engineeringtoolbox.com/gas-critical-temperature-pressure-d_161.html.
[59] "District heat prices | Helen," Apr. 2015. [Online]. Available: https://www.helen.fi/en/heating/district-heating/district-heat-prices.
[60] Kyrylo, "(2024) PPA price trends in Q1 2023. and where to find the best PPA deals in Europe? | Future Energy Go," Mar. 2023, [Online]. Available: https://futureenergygo.com/ppa-price-trends-in-q1-2023/.
[61] Motazedi K, Salkuyeh YK, Laurenzi IJ, MacLean HL, Bergerson JA. Economic and environmental competitiveness of high temperature electrolysis for hydrogen production. Int J Hydrogen Energy 2021;46(41):21274–88. https://doi.org/10.1016/j.ijhydene.2021.03.226.
[62] Lee S, et al. The effect of fuel utilization on heat and mass transfer within solid oxide fuel cells examined by three-dimensional numerical simulations. Int J Heat Mass Transf 2016;97:77–93. https://doi.org/10.1016/j.ijheatmasstransfer.2016.02.001.
[63] Büsch L, et al. HyPLANT100: industrialization from assembly to the construction site for gigawatt electrolysis. Hydrogen 2024;5(2):185–208. https://doi.org/10.3390/hydrogen5020012.
[64] Nayak-Luke RM, Bañares-Alcántara R. Techno-economic viability of islanded green ammonia as a carbon-free energy vector and as a substitute for conventional production. Energy Environ Sci 2020;13(9):2957–66. https://doi.org/10.1039/D0EE01707H.